# 4D Hyperspherical Harmonic (HyperSPHARM) Representation of Surface Anatomy: A Holistic Treatment of Multiple Disconnected Anatomical Structures

A. Pasha Hosseinbor*, Moo K. Chung, Stacey M. Schaefer, Carien M. van Reekum, Lara Peschke-Schmitz, Matt Sutterer, Andrew L. Alexander, Richard J. Davidson

***Abstract*— Multiple disconnected anatomical structures (MIDAS), such as the hippocampi and amygdalae in brain and the unfused hyoid bone in neck, are endemic to the human anatomy. Existing shape models, such as the widely used spherical harmonic (SPHARM) representation, are unable to represent MIDAS with a single mathematical parameterization. In such a situation, SPHARM has to be applied to each individual structure forming the MIDAS. In this paper, we present a novel surface parameterization technique using 4D *hyperspherical harmonics* (HSH) in representing compact, multiple disconnected anatomical structures as a single analytic function. The underlying idea behind the proposed hyperspherical harmonic representation (HyperSPHARM) is that any 3D object can be embedded onto the surface of a 4D hypersphere via stereographic projection. Extending the concept further, two or more disconnected 3D objects can be stereographically projected onto the same 4D hypersphere. If all the multiple disconnected 3D objects forming some MIDAS exist on the same hypersphere, then by Fourier analysis, the entire MIDAS can be parameterized by the 4D HSH. Hence, HyperSPHARM allows for a holistic treatment of MIDAS, unlike SPHARM. Another advantage of HyperSPHARM is that stereographic projection onto a hypersphere obviates the difficult 3D surface flattening required by SPHARM. We apply HyperSPHARM to the MIDAS comprising the left and right hippocampus and amygdala, and show that it achieves a far superior reconstruction using only 5 basis functions compared to SPHARM which requires more than 441.**

***Index Terms*— Hyperspherical Harmonics, SPHARM, Hippocampus & Amygdala, Shape Analysis**

## I. Introduction

Multiple disconnected anatomical structures (MIDAS) refer to two or more structures that are anatomically and/or functionally separate, and are endemic to the human anatomy. The underlying mathematical feature of MIDAS is changing topology, and prominent examples include the hippocampi and amygdalae in the brain and the unfused hyoid bone in the neck. Existing shape models, however, assume topological invarance, and so can only be applied to a single connected structure. An important problem then is formulating a single, coherent mathematical parameterization that can allow for a holistic treatment of MIDAS, i.e. treating the entire MIDAS as a single entity.

Probably the most widely applied shape parameterization technique for cortical structures is the spherical harmonic (SPHARM) representation [1]–[3], which has been mainly used as a data reduction technique for compressing global shape features into a small number of coefficients. The main global geometric features are encoded in low degree coefficients while the noise will be in high degree spherical harmonics. The method has been used to model various brain structures such as ventricles [2], hippocampi [3] and cortical surfaces [1]. SPHARM, however, can't represent MIDAS with a single parameterization. In such a situation, SPHARM has to be applied to each individual structure forming the MIDAS. In addition, SPHARM-representation requires a 3D anatomical surface to be mapped onto a 3D sphere, which is no simple task. Various computationally intensive surface flattening techniques have been proposed as a result: diffusion mapping [1], conformal mapping [4], and area preserving mapping [2]. The surface flattening is used to parameterize the surface using two spherical angles. The angles serve as coordinates for representing the surface using spherical harmonics. Then the surface coordinates can be mapped onto the sphere and each coordinate is represented as a linear combination of spherical harmonics.

Any 3D object can be embedded onto the surface of a 4D hypersphere via simple stereographic projection. Extending the concept further, two or more disconnected 3D objects can be stereographically projected onto the same 4D hypersphere. Consequently, all the multiple disconnected 3D objects (forming the MIDAS) exist on the same hypersphere, and so the entire MIDAS can be represented as the linear combination of 4D hyperspherical harmonics (HSH), which are the multidimensional analogues of the 3D spherical harmonics. In other words, such a procedure enables the entire MIDAS to be treated as a single entity existing along the surface of a 4D hypersphere.

The HSH have been mainly confined to quantum chemistry, where their utility first became evident with respect to solving the Schrödinger equation for the hydrogen atom. It had



Manuscript received October 31, 2006; revised July 18, 2007 *Asterisk indicates corresponding author.*

M.K. Chung is with the Department of Biostatistics and Medical Informatics, and the Waisman Laboratory for Brain Imaging and Behavior, University of Wisconsin, Madison, WI 53706 (e-mail: mkchung@wisc.edu).

K. M. Dalton and R. J. Davidson are with the Waisman Laboratory for Brain Imaging and Behavior, University of Wisconsin, Madison.

been solved in position-space by Schrödinger, himself, but not in momentum-space, which is related to position-space via the Fourier transform. Sometime later, V. Fock solved the Schrödinger equation for the hydrogen atom directly in momentum-space. In his classic paper [5], Fock stereographically projected 3D momentum-space onto the surface of a 4D unit hypersphere, and after this mapping was made, he was able to show that the eigenfuctions were the 4D HSH. Recently, the HSH have been utilized in a wider array of fields than just quantum chemistry, including computer graphics visualization [6] and crystallography [7]. However, as of yet, they have remained elusive for medical imaging.

In this paper, following the approach of Fock, we model multiple disconnected 3D objects in terms of the 4D HSH by stereographically projecting each object's surface coordinates onto the same 4D hypersphere, and label such a representation HyperSPHARM [8]. The incorporation of an extra ($4^{th}$) dimension imbues HyperSPHARM with several key advantages over SPHARM:

1) Stereographic projection onto a 4D hypersphere obviates the difficult and time-consuming 3D surface flattening required by SPHARM.
2) HyperSPHARM treats MIDUS holistically by representing it with a single (linear) mathematical parameterization, given by the 4D HSH. SPHARM, however, has to be applied to each individual structure forming the MIDAS.
3) HyperSPHARM possess robust reconstruction accuracy using only a few basis functions, which we will demonstrate. In fact, we will show that HyperSPHARM achieves superior reconstruction using only a fraction of the fitting parameters expended by SPHARM to achieve a comparable reconstruction.

The method is applied to modeling the MIDAS comprising the left and right hippocampus and amygdala, and we compare to SPHARM.

## II. 4D Hyperspherical Harmonics

Consider the 4D unit hypersphere $S^3$ existing in $\mathbb{R}^4$. The Laplace-Beltrami operator on $S^3$ is defined as

$$\Delta_{S^3} = \frac{1}{\sin^2\beta}\frac{\partial}{\partial\beta}\sin^2\beta\frac{\partial}{\partial\beta} + \frac{1}{\sin^2\beta}\Delta_{S^2}, \tag{1}$$

where $\Delta_{S^2}$ is the Laplace-Beltrami operator on the unit sphere $S^2$. The eigenfuctions of Eq. (1) are the 4D hyperspherical harmonics $Z_{nl}^m(\beta,\theta,\phi)$:

$$\Delta_{S^3} Z_{nl}^m = -l(l+2)Z_{nl}^m.$$

The 4D HSH are defined as [9]

$$Z_{nl}^m(\beta,\theta,\phi) = 2^{l+1/2}\sqrt{\frac{(n+1)\Gamma(n-l+1)}{\pi\Gamma(n+l+2)}}\Gamma(l+1)\sin^l\beta C_{n-l}^{l+1}(\cos\beta)\,Y_l^m(\theta,\phi) \tag{2}$$

where $(\beta,\theta,\phi)$ obey ($\beta\in[0,\pi], \theta\in[0,\pi], \phi\in[0,2\pi]$), $C_{n-l}^{l+1}$ are the Gegenbauer (ultraspherical) polynomials, and $Y_l^m$ are the 3D spherical harmonics. The index $l$ denotes the degree of the HSH, $m$ is the order, and $n = 0, 1, 2, ...$, and these three integers obey the conditions $0 \le l \le n$ and $-l \le m \le l$. The number of HSH corresponding to a given value of $n$ is $(n+1)^2$. The first few 4D HSH are shown in Table I. The HSH form an orthonormal basis on the hypersphere, and the normalization condition reads

$$\int_0^{2\pi}\int_0^{\pi}\int_0^{\pi} Z_{nl}^m(\beta,\theta,\phi)Z_{n'l'}^{m'*}(\beta,\theta,\phi)\sin^2\beta\sin\theta d\beta d\theta d\phi = \delta_{nn'}\delta_{ll'} \tag{3}$$

TABLE I: List of a F

| | |
|---|---|
| $Z_{00}^0(\beta,\theta,\phi) = \frac{1}{\pi\sqrt{2}}$ | $Z_1^0$ |
| $Z_{11}^{-1}(\beta,\theta,\phi) = \frac{-\sqrt{2}}{\pi}\sin\beta\ \sin\theta\ \sin\phi$ | $Z_1^0$ |
| $Z_{11}^{1}(\beta,\theta,\phi) = \frac{-\sqrt{2}}{\pi}\sin\beta\ \sin\theta\ \cos\phi$ | $Z_2^0$ |
| $Z_{21}^{-1}(\beta,\theta,\phi) = \frac{-\sqrt{3}}{\pi}\sin 2\beta\ \sin\theta\ \sin\phi$ | $Z_2^0$ |

## III. HyperSPHARM Algorithm

In this section, we will elaborate on the HyperSPHARM algorithm, which consists of four basic steps: translation, stereographic projection, 4D HSH expansion, and linear least squares estimation. Before proceeding, we need to define our MIDAS.

Suppose some MIDAS is composed of $k$ individual structures. Each structure is assumed to be both 3D finite and compact (i.e. has no singularities) and comprising surface coordinates $\mathbf{p}_j = (\mathbf{p}_j^1\ \mathbf{p}_j^2\ \mathbf{p}_j^3)$, where $j = 1, 2, ..., k$. We further assume that each structure consists of $N_j$ mesh vertices, which means the dimension of $\mathbf{p}_j$ is $N_j$ x 3. Lets combine the surface coordinates of all $k$ structures in order to facilitate a holistic treatmeant of the MIDAS. Define $\mathbf{v} = (\mathbf{v}^1\ \mathbf{v}^2\ \mathbf{v}^3)$ as the combined 3D surface coordinates across all $k$ structures, where $\mathbf{v}^1 = (\mathbf{p}_1^{1T}\ \mathbf{p}_2^{1T}\ \cdots\ \mathbf{p}_k^{1T})^T$, $\mathbf{v}^2 = (\mathbf{p}_1^{2T}\ \mathbf{p}_2^{2T}\ \cdots\ \mathbf{p}_k^{2T})^T$, and $\mathbf{v}^3 = (\mathbf{p}_1^{3T}\ \mathbf{p}_2^{3T}\ \cdots\ \mathbf{p}_k^{3T})^T$ and the symbol $T$ denotes transpose. In other words, the MIDAS's surface coordinates are defined by $\mathbf{v}$. The dimension of $\mathbf{v}$ is $M$ x 3, where $M = \sum_{j=1}^k N_j$ is the total number of mesh vertices comprising the 3D MIDAS. We denote each (vector) coordinate component of $\mathbf{v}$ as $\mathbf{v}^i$, where $i = 1, 2, 3$.

### A. Translation

Translating the MIDAS's surface coordinates $\mathbf{v}$ closer to the origin $(0,0,0)$ ... We achive this shift towards the origin by subtracting each $\mathbf{v}^i$ by its mean value:

$$\mathbf{s}^i = \mathbf{v}^i - \langle\mathbf{v}^i\rangle,$$

where $\mathbf{s} = (\mathbf{s}^1\ \mathbf{s}^2\ \mathbf{s}^3)$ is the $M$ x 3 matrix denoting the MIDAS's shifted surface coordinates and $\langle\mathbf{v}^i\rangle$ is the mean of $\mathbf{v}^i$. The translation serves to ...

### B. Stereographic Projection of 3D MIDAS's Surface Coordinates onto 4D Hypersphere

In order to model the MIDAS's (shifted) surface coordinates with the HSH, we need to map them onto a 4D hypersphere, which can be achieved via stereographic projection

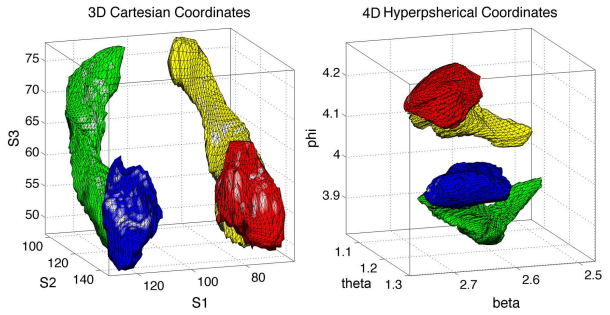


Fig. 1: The 3D subcortical structures (left) in the coordinates $(v^1, v^2, v^3)$ went through the 4D stereographic projection that resulted in conformally deformed structures (right) in the 4D spherical coordinates $(\beta, \theta, \phi)$. The 3D subcortical structure is then embedded on the surface of the 4D hypersphere with radius $p_o = 12000$, which makes the surface of the hypersphere to be almost Euclidean.

[5]. The surface coordinates in 3D spherical space are $s^1 = r\sin\theta\cos\phi$, $s^2 = r\sin\theta\sin\phi$, and $s^3 = r\cos\theta$, where $r = \sqrt{(s^1)^2 + (s^2)^2 + (s^3)^2}$. Consider a 4D hypersphere of radius $p_o$, whose coordinates are defined as

$$\begin{aligned} u_1 &= p_o \sin\beta\sin\theta\cos\phi \\ u_2 &= p_o \sin\beta\sin\theta\sin\phi \\ u_3 &= p_o \sin\beta\cos\theta \\ u_4 &= p_o \cos\beta. \end{aligned}$$

The relationship between $(s^1, s^2, s^3)$ and $(u_1, u_2, u_3, u_4)$, according to stereographic projection, is

$$u_1 = \frac{2p_o^2 s^1}{r^2 + p_o^2}, \quad u_2 = \frac{2p_o^2 s^2}{r^2 + p_o^2}, \quad u_3 = \frac{2p_o^2 s^3}{r^2 + p_o^2}, \quad u_4 = \frac{p_o(r^2 - p_o^2)}{r^2 + p_o^2} \tag{4}$$

According to Eq. (4), the coordinate $(0, 0, 0)$ projects onto the south pole $(0, 0, 0, -p_o)$ of the hypersphere. As $r \to \infty$, the projection $(u_1, u_2, u_3, u_4)$ moves closer to the north pole $(0, 0, 0, p_o)$ of hypersphere. Thus, the north pole is not associated with any $(s^1, s^2, s^3)$, but gives us a way of envisioning infinity as a point. Eq. (4) establishes a one-to-one correspondence between the 3D volume and 4D hypersphere (Figure 1).

Stereographic projection exhibits two important properties. First, it is conformal, which means it preserves angles - the angles $(\theta, \phi)$ defining the 3D surface are preserved in 4D hyperspherical space. Second, stereographic projection does not preserve volume; in general, the volume of a region in the 3D plane doesn't equal the volume of its projection onto the hypersphere. However, such volume distortion only arises when mathematical integration over surfaces is involved. Since the HyperSPHARM algorithm does not employ integration of any kind, steographic projection's inherent lack of volume preservation will not be an issue in the surface reconstructions.

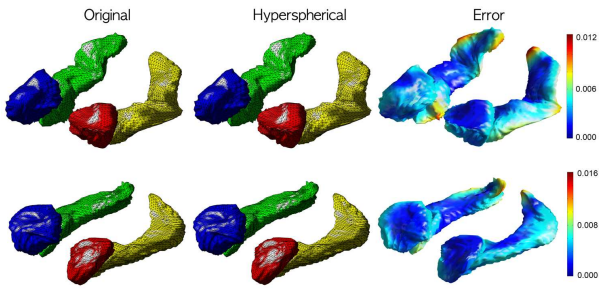


Fig. 2: Hyperspherical harmonic representation of amygdala and hippocampus surfaces for subject 10 and 60. The vertex-wise reconstruction errors are also plotted. As expected, most errors are occurring near sharp peaks and corners.

### C. HSH Expansion of MIDAS's Surface Coordinates

Stereographically projecting the 3D MIDAS's surface coordinates onto a 4D hypersphere results in them existing along the hypersphere's surface. According to Fourier analysis, any square-integrable function defined on a sphere can be expanded in terms of the spherical harmonics. Thus, we can expand each coordinate component $s^i$ in terms of the 4D HSH:

$$s^i_{p_o}(\beta, \theta, \phi) \approx \sum_{n=0}^{N} \sum_{l=0}^{n} \sum_{m=-l}^{l} C^i_{nlm} Z^m_{nl}(\beta, \theta, \phi), \tag{5}$$

where $s^i_{p_o}$ denotes the $i^{th}$ component of the surface coordinates $\mathbf{s}$ existing on hypersphere of radius $p_o$. The realness of the surface coordinates requires use of the real HSH, and so we employ a modified real basis used in [10] for $Y^m_l$. $N$ is the truncation order of the HSH expansion, and for a given $N$ the total number of HSH expansion coefficients is $W = (N+1)(N+2)(2N+3)/6$.

### D. Numerical Implementation

Let $\Omega_j = (\beta_j, \theta_j, \phi_j)$ denote the hyperspherical angles at the $j$-th mesh vertex. Recall that our MIDAS consists of a total of $M$ mesh vertices, and so each $\mathbf{s}^i$ is a $M$ x 1 vector. Denote $\mathbf{C}^i$ as the $W$ x 1 vector of unknown HSH expansion coefficients $C^i_{nlm}$ for each $\mathbf{s}^i$, and $\mathbf{A}$ the $M$ x $W$ matrix constructed with the HSH basis

$$\mathbf{A} = \begin{pmatrix} Z^0_{00}(\Omega_1) & Z^0_{10}(\Omega_1) & Z^{-1}_{11}(\Omega_1) & Z^0_{11}(\Omega_1) & \cdots & Z^N_{NN}(\\ \vdots & \vdots & \vdots & \vdots & \ddots & \vdots \\ Z^0_{00}(\Omega_M) & Z^0_{10}(\Omega_M) & Z^{-1}_{11}(\Omega_M) & Z^0_{11}(\Omega_M) & \cdots & Z^N_{NN}(\Omega \end{pmatrix}$$

Thus, the general linear system representing Eq. (5) is described by $\mathbf{s}^i = \mathbf{A}\mathbf{C}^i$. This system of over-determined equations is solved via linear least squares, yielding

$$\widehat{\mathbf{C}^i} = (\mathbf{A}^T\mathbf{A})^{-1}\mathbf{A}^T\mathbf{s}^i \tag{6}$$

The reconstructed (shifted) surface coordinates are then given by $\widehat{\mathbf{s}^i} = \mathbf{A}\widehat{\mathbf{C}^i}$.

Lastly, we want to estimate the actual surface coordinates $\mathbf{v}$. The reconstructed $\mathbf{v}^i$ is

$$\widehat{\mathbf{v}^i} = \widehat{\mathbf{s}^i} + \langle \mathbf{v}^i \rangle, \tag{7}$$

where we have translated the reconstructed (shifted) surface coordinates back to the original object space. Hence, our reconstructed 3D MIDAS is defined by the $M$ x 3 matrix $\widehat{\mathbf{v}} = (\widehat{\mathbf{v}^1}\ \widehat{\mathbf{v}^2}\ \widehat{\mathbf{v}^3})$. The mean squared error (MSE) between the original MIDAS and the HyperSPHARM-reconstructed MIDAS can then be computed as

$$\text{MSE} = \text{tr}\big[(\mathbf{v} - \widehat{\mathbf{v}})^T(\mathbf{v} - \widehat{\mathbf{v}})\big]/M \tag{8}$$

## IV. Experimental Results and Applications

We collected high-resolution T1-weighted inverse recovery fast gradient echo MRI in 124 contiguous 1.2-mm axial slices (TE=1.8 ms; TR=8.9 ms; flip angle = 10°; FOV = 240 mm; 256 × 256 data acquisition matrix) of 69 middle-age and elderly adults ranging between 38 to 79 years (mean age = 58.0 ± 11.4 years). The data were collected as a part of a national study called MIDUS (Midlife in US; `http://midus.wisc.edu`) for the health and well-being in the aged population [11]. There are 23 men and 46 women in the study. Brain tissues in the MRI scans were automatically segmented using Brain Extraction Tool (BET) [12] and trained raters manually segmented the parts of limbic system: amygdala and hippocampus. A nonlinear image registration using the diffeomorphic shape and intensity averaging technique with the cross-correlation as the similarity metric through Advanced Normalization Tools (ANTS) [13] was performed and the study specific template is constructed. The isosurfaces of the segmentation were extracted using the marching cube algorithm (Figure 2).

### A. Selection of Optimal $p_o$

Choosing the optimal $p_o$ for HyperSPHARM reconstruction can be determined by plotting the MSE versus $p_o$ for the entire MIDAS reconstruction. Note the analysis is done on the mean population template instead of each individual subject so to minimize inter-subject variability. The HSH of truncation order $N = 1$ are used for the HyperSPHARM reconstruction of the template. Fig. 3 displays plot of the MSE of each $\mathbf{v}^i$ as a function of $p_o$ for the entire MIDAS reconstruction, indicating that the MSE decreases as the hypersphere radius increases. A $p_o \geq 8000$ guarantees the MSE of each $\mathbf{v}^i$ to be less than $10^{-9}$. Such small mean squared errors across a wide range of radii is indicative of the robust reconstruction accuracy of HyperSPHARM and gives much flexiblity in the selection of $p_o$. We employ $p_o = 12000$ for our analysis.

### B. HyperSPHARM Reconstructions and Comparison to SPHARM Representation

HyperSPHARM was used to reconstruct the MIDAS comprising the left and right hippocampus and amygdala for 69 subjects. For the entire MIDAS, the HyperSPHARM parameters were radius $p_o = 12000$ and $N = 1$, which results in $W = 5$ HSH expansion coefficients for each $s^i$. So total of 15 HSH coefficients can parameterize the entire MIDAS. SPHARM has

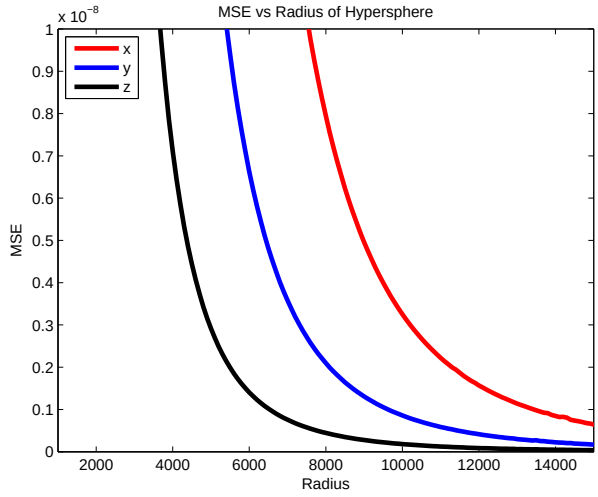


Fig. 3: Plot of the MSE as a function of the hypersphere radius $p_o$ for MIDAS comprising the left and right hippocampus and amygdala. Note that the analysis is done on the mean population template. The HSH of truncation order $N = 1$ are used for the HyperSPHARM reconstruction of template, which means only $W = 5$ HSH expansion coefficients are expended for each $\mathbf{v}^i$. The plot shows that the MSE is very small across a wide range of radii: an order of magnitude of $10^{-9}$ or smaller for the entire MIDAS reconstruction.

| | SPHARM 2 | SPHARM 10 | SPHARM 20 | H |
|---|---|---|---|---|
| Left Amygdala | 1.08 ± 0.17 | 0.054 ± 0.010 | 0.022 ± 0.005 | 0.18 ± 0 |
| Right Amygdala | 0.60 ± 0.11 | 0.052 ± 0.008 | 0.023 ± 0.003 | 0.27 ± 0 |
| Left Hippocampus | 1.77 ± 0.33 | 0.127 ± 0.026 | 0.043 ± 0.040 | 0.90 ± 0 |
| Right Hippocampus | 1.08 ± 0.17 | 0.054 ± 0.010 | 0.022 ± 0.005 | 0.18 ± 0 |

TABLE II: The mean squared error (MSE) and its standard deviation of reconstruction. MSE is computed over all mesh vertices and averaged over 69 subjects. Degree 2, 10 and 20 SPHARM representations require $3^2 = 9, 11^2 = 121$ and $21^2 = 441$ basis functions, respectively. The reconstruction error of HSH expansion of order $N = 1$ is substantially smaller than those of SPHARM, even though only 5 HSH basis functions are used.

to be applied to each individual structure forming the MIDAS. Thus, for a SPHARM representation of order $L$, a total of $3(L+1)^2$ expansion coefficients parameterize a single structure and $12(L+1)^2$ coefficients all four disconnected surfaces (i.e. left and right hippocampus and amygdala).

Figure 2 shows the HyperSPHARM-reconstructed surfaces for two different subjects. The length of the residual is computed and plotted on the reconstructed surfaces. The reconstructions are nearly identical to the originals, with very small erros. As expected, most reconstruction errors are found near the surfaces' peaks and corners.

We have compared the reconstruction errors between HSH and SPHARM representations. Hippocampus and amygdala surface meshes are flattened to a unit sphere and resampled to a uniform grid along the sphere. Then degree 2, 10 and 20

SPHARM representations are constructed. The MSE of each reconstruction is computed within each surface and averaged over 69 subjects (Table II). Its standard error is also computed over all 69 subjects.

The degree 2, 10 and 20 SPHARM representations require 9, 121 and 441 basis functions. Even with only 5 basis functions, HSH is achieving substantially low MSE compared with SPHARM reconstruction with 441 basis functions, demonstrating the superior efficiency in the HSH representation.

### C. Influence of Age and Gender

HSH representations were obtained for hippocampus and amygdala surfaces of all 69 subjects. The representation behaves like surface smoothing technique where high frequency noise is removed as shown in Figure 2. The 69 reconstructed surfaces are then averaged to produce the population specific template. The 3D displacement vector field from the template to individual surface is taken as the response vector in the multivariate general linear model (MGLM) [1] and its $T$-statistic is computed and thresholded at $p < 0.05$. The random field based multiple comparisons are performed to give stringent results. We have detected significant influence of age mainly on the tail regions of the hippocampus while there is no influence of gender on any of the structures.

## V. Discussion

Studying the development of anatomical structures over time ... Consider the case of the hyoid bone, which at birth consists of three disjoint components, but which will eventually fuse together at around age 40. In other words, before the age of 40 the hyoid bone constitutes a MIDAS, but then develops into a single connected surface. In a developmental study on the hyoid bone then, this evolution from a MIDAS to a single connected structure would not be an issue in terms of HyperSPHARM surface reconstruction because of its ability to treat multiple disjoint structures as a single entity. In SPHARM's case, however, it will initially parameterize three different structures (i.e. components of unfused hyoid bone), but eventually only a single structure once the components have fused. Consequently, the exact transition point from unfused to fused will have to be taken into account for the SPHARM reconstruction of hyoid bone.

## VI. Conclusion and Discussion

In this paper, we have presented a new analytic approach for representing multiple disconnected shapes using a single analytic function, which is a linear combination of HSH. The method is applied to parameterizing 4 disconnected subcortical structures (two amygdalae and two hippocampi) using only 60 HSH coefficients. The resulting HSH coefficients are global and contain information about all four structures, so they do not provide any local shape information. Therefore, HyperSPHARM might be better suited to sparse techniques such as wavelets, which will be explored in future. Despite HSH being a global basis, by reconstructing surfaces at each voxel and using HSH as a way to filter out high frequency noise, it was possible to use HSH for local inference at vertex level as shown in our application. Although the individual image volumes are registered to a template using diffeomorphic warping [13], we might only need an affine registration to initially align the structures and simply match the coefficients as in SPHARM [1] but the issue is not explored here and left as a future study.

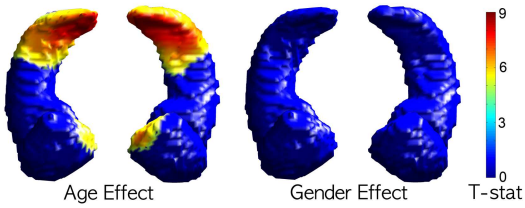


Fig. 4: The regions showing statistically significant age effect thresholded at $p < 0.05$ (corrected). There is no gender effect.

**Acknowledgements.** This research was supported by the National Institute of Aging (P01-AG20166) and National Institute on Mental Health (R01 MH043454). Seung-Goo Kim of Max Planck Institutes performed image registration.

## References

[1] M. Chung, K. Worsley, M. Brendon, K. Dalton, and R. Davidson, "General multivariate linear modeling of surface shapes using SurfStat," *NeuroImage*, vol. 53, pp. 491–505, 2010.

[2] G. Gerig, M. Styner, D. Jones, D. Weinberger, and J. Lieberman, "Shape analysis of brain ventricles using spharm," in *MMBIA*, 2001, pp. 171–178.

[3] L. Shen, J. Ford, F. Makedon, and A. Saykin, "surface-based approach for classification of 3d neuroanatomical structures," *Intelligent Data Analysis*, vol. 8, pp. 519–542, 2004.

[4] S. Angenent, S. Hacker, A. Tannenbaum, and R. Kikinis, "On the laplace-beltrami operator and brain surface flattening," *IEEE Transactions on Medical Imaging*, vol. 18, pp. 700–711, 1999.

[5] V. Fock, "Zur theorie des wasserstoffatoms," *Z. Physik*, vol. 98, pp. 145–154, 1935.

[6] B. Bonvallet, N. Griffin, and J. Li, "3D shape descriptors: 4D hyperspherical harmonics 'An exploration into the fourth dimension'," in *IASTED International Conference on Graphics and Visualization in Engineering*, 2007, pp. 113–116.

[7] J. K. Mason and C. A. Schuh, "Hyperspherical harmonics for the representation of crystallographic texture," vol. 56, pp. 6141–6155, 2008.

[8] A. P. Hosseinbor, M. K. Chung, S. M. Schaefer, van Reekum C. M., L. Peschke-Schmitz, M. Sutterer, A. L. Alexander, and R. J. Davidson, "4D hyperspherical harmonic (HyperSPHARM) representation of multiple disconnected brain subcortical structures," in *MICCAI*, 2013.

[9] G. Domokos, "Four-dimensional symmetry," *Physical Review*, vol. 159, pp. 1387–1403, 1967.

[10] C. G. Koay, E. Ozarslan, and P. J. Basser, "A signal transformational framework for breaking the noise floor and its applications in MRI," *J. Magn. Reson.*, vol. 197, pp. 108–119, 2009.

[11] C. Van Reekum, S. Schaefer, R. Lapate, C. Norris, L. Greischar, and R. Davidson, "Aging is associated with positive responding to neutral information but reduced recovery from negative information," *Social Cognitive and Affective Neuroscience*, vol. 6, pp. 177–185, 2011.

[12] S. Smith, "Fast robust automated brain extraction," *Human Brain Mapping*, vol. 17, pp. 143–155, 2002.

[13] B. Avants, C. Epstein, M. Grossman, and J. Gee, "Symmetric diffeomorphic image registration with cross-correlation: Evaluating automated labeling of elderly and neurodegenerative brain," *Medical image analysis*, vol. 12, pp. 26–41, 2008.